Investigations of Electrospray Sample Deposition for Polymer MALDI Mass Spectrometry

Scott D. Hanton, Ingrid Z. Hyder, and James R. Stets
Air Products and Chemicals, Inc., Allentown, Pennsylvania, USA

Kevin G. Owens
Department of Chemistry, Drexel Univiersity, Philadelphia, Pennsylvania, USA

William R. Blair and Charles M. Guttman
Polymers Division, National Institute of Standards and Technology, Gaithersburg, Maryland, USA

Anthony A. Giuseppetti
American Dental Association Health Foundation-Paffenbarger Research Center, Gaithersburg, Maryland, USA

In the interest of a more thorough understanding of the relationship between sample deposition technique and the quality of data obtained using matrix-assisted laser desorption/ionization (MALDI) mass spectrometry, details of the electrospray (ES) process of sample deposition are investigated using a number of techniques. Sample morphology was observed with scanning electron microscopy (SEM) and atomic force microscopy (AFM), while matrix-enhanced secondary ion mass spectrometry (MESIMS) monitored surface coverage. Electrospray deposition reduces the analyte segregation that can occur during traditional dried droplet deposition for MALDI. We attribute statistically significant improvements in the reproducibility of signal intensity and MALDI average molecular mass measurements to the ES sample deposition technique. (J Am Soc Mass Spectrom 2004, 15, 168−179) © 2004 American Society for Mass Spectrometry

Matrix-assisted laser desorption/ionization (MALDI) mass spectrometry techniques [1–4] have been developed to determine the chemical structure of a variety of industrial polymers [5, 6]. Important information that can be determined includes the monomer mass, end group mass, and molecular mass distribution (including the number-average molecular mass, M_N, the mass-average molecular mass, M_W, and the polydispersity, PD). [According to ISO 31-8, the term "Molecular Weight" has been replaced by "Relative Molecular Mass", symbol M_r. Thus, if this nomenclature and notation were to be followed in this publication, one would write $M_{r,n}$ instead of the historically conventional M_n for the number average molecular weight, with similar changes for M_w, M_z and M_v, and it would be called the "Number Average Relative Molecular Mass". The conventional notation, rather than the ISO notation, has been employed for this publication.] The chemical structure of a polymer directly influences many polymer physical properties: tensile strength, elongation, brittleness, abrasion resistance, chemical resistance, viscosity, adhesion, and solubility [7].

Since the introduction of MALDI, the development of reliable sample preparation methods has been critical to the success of MALDI experiments. Reliable MALDI sample preparation requires correct choice of the solvent system, the matrix, and the ionization reagent. Successful MALDI sample preparation is challenged by the chemical diversity of synthetic polymers. It has been shown that the rate of solvent evaporation plays a significant role in the sample preparation [8]. Electrospray (ES) sample deposition has been demonstrated to markedly improve the homogeneity of the MALDI sample surface [9], improve signal strength and repeatability [10], and enable the use of MALDI in quantitative analysis of several peptide drugs [11].

In these experiments we examined the morphology and surface coverage of the ES-deposited samples by SEM [12], AFM [13], and MESIMS [9, 14, 15]. These tools were used to better understand the coverage of the ES sample, and the impact of spray time and spray distance. We also investigated the robustness (degree of

Published online December 9, 2003

Address reprint requests to Dr. S. D. Hanton, Air Products and Chemicals, Inc., 7201 Hamilton Blvd., Allentown, PA 18195, USA. E-mail: HantonSD@APCI.com

1044-0305/04/$30.00
doi:10.1016/j.jasms.2003.09.012

Received January 8, 2003
Revised September 15, 2003
Accepted September 28, 2003

non-interaction and non-penetration) of sprayed layers using MESIMS and MALDI.

SEM and AFM are both well-developed microscopy techniques, each with very high spatial resolving power. They differ in some important ways, however, and thus provide complementary information [16].

In SEM, an electron beam is produced by either thermionic or field emission from an electron gun. The electron column which houses the gun, lenses, and specimen chamber is under vacuum, typically 10^{-7} to 10^{-9} torr. The electron beam is focused via a series of lenses and apertures to a fine probe, which varies from nanometers to micrometers, depending on operating conditions. When the beam impinges on a specimen, the interaction of the primary beam electrons with the atoms in the specimen generates secondary electrons, the intensity of which is dependent on the sample topography. A second electron beam moves across the CRT display in synchrony with the electron probe's movement across the surface of the specimen, resulting in a real-time secondary electron image. SEM images are easy to interpret, the instrument has a large depth of field, and minimal sample preparation is required in most cases.

In AFM, a sharp silicon probe (with an end radius of about 10 nm) mounted on a microscopic cantilever is scanned across the specimen by a piezoelectric tube scanner. The scanner is capable of rastering (scanning in x and y, similar to the electron beam in SEM) and also extending and retracting (in z). Simultaneously, a laser is reflected from the top of the cantilever to a position-sensitive diode detector. Differences in surface height cause the cantilever to deflect and the beam to move away from its setpoint; in response, the piezoelectric scanner extends or retracts to return to the setpoint. The information from this feedback loop is used to construct topographic maps of the sample surface, i.e., two-dimensional arrays of height data. The two most common modes of imaging are contact mode and tapping mode. In the former, a constant force is maintained between tip and sample by extending or retracting the scanner. In tapping mode, the cantilever is oscillated at its resonant frequency, and a specified amount of amplitude damping is maintained by extension or retraction of the scanner. The height corresponding to the setpoint amplitude is recorded at every point in the image, and this provides the "map". Tapping mode has the advantage of significantly reduced lateral forces during imaging.

In contrast to SEM, AFM is usually conducted under ambient pressure. This can be an advantage when a sample might be altered by exposure to vacuum. Another difference between the techniques is the ability of AFM to quantitate heights. An AFM "image" is really an array of height values and therefore contains quantitative height information, which can be easily extracted. In SEM, there is no straightforward way of measuring height values. A strength of SEM compared to AFM is its significantly greater depth of field, which can be on the order of millimeters, while AFM has a maximum range of few micrometers. A fourth difference between the techniques is the susceptibility of AFM images to tip artifacts. Because images are constructed through the interaction of a physical probe and the surface of interest, changes in the probe or even the finite size of the probe itself can introduce artificial elements in the images. In contrast, SEM is free from tip artifacts. In this study, we have used the complementary advantages of both techniques to fully characterize the spray-deposited samples.

Traditional dried droplet MALDI experiments have been plagued by sample heterogeneity that results in significant spot-to-spot variation in the ion intensity. We expected that this heterogeneity may significantly impact the precision of average molecular mass measurements on polymer samples as well as other MALDI experiments, such as accurate mass determination and chemical structure determination by post source decay (PSD). To investigate the ability of ES deposition to improve the precision of polymer MALDI average molecular mass measurements, we have analyzed low mass polymers prepared from different matrices, with both ES- and dried droplet deposition. The results demonstrate a statistically significant improvement in the precision of average molecular mass measurements with the use of electrospray deposition compared with dried droplet deposition.

Experimental

NIST Disclaimer: Certain commercial materials and equipment are identified in this paper in order to specify adequately the experimental procedure. In no case does such identification imply recommendation or endorsement by the National Institute of Standards and Technology, nor does it imply necessarily the best available for the purpose.

Materials

The following polymers were used in the investigations described herein : Polystyrene (PS), Poly(ethylene glycol) (PEG), and Poly(methyl methacrylate) (PMMA), obtained from Polymer Source, (Dorval, Quebec, Canada), Aldrich, (Milwaukee, WI), and Polymer Standards Service, (Mainz, Gremany), respectively. The matrix compounds dithranol and 2,5-dihydroxybenzoic acid were obtained from Aldrich. Silver trifluoroacetate, Aldrich, was used with polystyrene samples as an ionization reagent. The solvents tetrahydrofuran and acetonitrile, used in sample solution preparation, were obtained from North Strong Scientific, (Phillipsburg, PA). Deionized water of 15 to 18 megaohm resistivity was obtained from an Aqua-Summa reagent water system (U.S. Filter/Culligan, Beltsville, MD).

The azodyes used in this work were synthesized by Dr. Shashadhar Samal while he was in the Department of Chemistry at Ravenshaw College, Cuttack–753 003,

India [17]. These syntheses followed procedures established by Szele and Zollinger [18]. The azodyes used as matrices contain from two to four aromatic rings. The compound found to be most useful as a matrix was prepared by coupling a diazonium salt of 4,4′-diaminodiphenylmethane with phenol. The structure for this compound is shown in Scheme **1**.

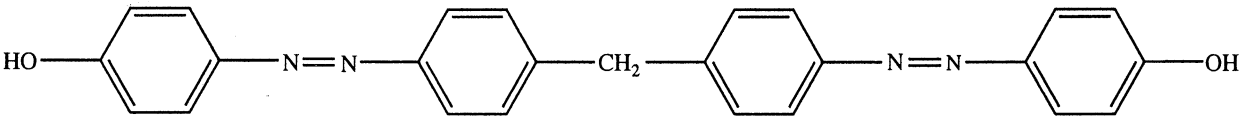

Scheme 1. Chemical structure of an azodye matrix.

Sample Preparation for Microscopy of ES Samples

Wet polymer MALDI sample preparation usually involves mixing an analyte solution (typically 5 mg/mL for low mass analytes) and a matrix solution (typically between 0.10 to 0.25 M or 23 to 57 mg/mL with dithranol , FW = 226.23, as an example). For a 0.25 M matrix solution, the analyte and matrix solutions are mixed 1:7 by volume. For Na^+ cationization, sufficient Na is usually obtained by preparing samples in soft glass vials. For Ag^+ cationization, a volume equal to the analyte solution of a 5 mg/mL solution of AgTFA is mixed with the matrix solution. For dried droplet samples (0.3 to 2.0) μL are deposited on the sample substrate and allowed to dry.

ES samples are deposited using a home-built ES deposition apparatus constructed from a Harvard Apparatus model 22 infusion pump (Harvard Apparatus, Inc., Holliston, MA) and a custom-built high voltage power supply (based on a Bertan, Inc. model PMT-75C-P-3 0 250 uA precision PMT power supply module, output voltage 0–7.5 kV). The ES needle is a 100 mm length of 1.6 mm o.d. by 0.25 mm i.d. stainless steel HPLC tubing (Alltech, Inc., Deerfield, IL) mounted in a delrin holder. A 100 uL gas-tight syringe (Hamilton, Inc., Reno, NV) mounted in the infusion pump is connected to the ES needle by an approximately 0.5 m length of 0.125 mm i.d. PEEK tubing using PEEK zero-dead volume unions (Upchurch Scientific, Inc., Oak Harbor, WA). Note that the PEEK tubing is replaced with Teflon tubing for use with solvents such as THF. In a typical experiment, approximately 20 μL of the premixed sample solution is loaded into the ES needle. The sample flows at a rate of approximately 2 to 3 μL per min while a potential of approximately +5 to +7 kV is applied to the needle. Typical spray times are 30 s to two min. When the sample substrate is held at ground a distance of 15 to 25 mm away, a circular spray pattern is created approximately 2 to 2.5 cm in diameter. While almost any conducting surface can be used as an ES deposition substrate, we chose front surface aluminum mirrors (Edmund Scientific, Barrington, NJ) for the samples examined by SEM, AFM, and MESIMS. The optically flat substrate ensured that any observed variations were due to the sample, not the substrate. ES deposition method development (for different sample/solvent combinations and chosen spray distance) involves adjustment of the flow rate and applied voltage in order to obtain a stable, elongated Taylor cone.

Sample Preparation for MALDI Signal Repeatability Studies

Samples were prepared by one of two methods, either deposited by dried droplet or electrosprayed onto a stainless steel target substrate. Approximately 0.3 to 0.5 μL of solution per sample site was placed on the target when samples were prepared by dried droplet. It was helpful to view the target through a stereo microscope (Fisher Scientific, Pittsburg, PA) while depositing the sample solution onto the target. Solution was delivered to the surface using a 5 μL glass capillary pipette (Drummond Scientific, Broomall, PA). Solvent was evaporated at room temperature in still air. No additional measures were taken to speed up or slow the solvent evaporation.

An electrospray apparatus was assembled from the following components: an adjustable, high-voltage power supply with a voltage range of 0 to 10 kV (Spellman High Voltage Electronics Corp., Hauppauge, NY), a Harvard model 22 syringe pump (Harvard Apparatus, Inc., Holliston, MA) and a manually adjusted x-y-z positioning movement (Edmund Scientific, Barrington, NJ). The syringe pump and x-y-z- positioning movement were mounted on a small (20.3 cm $\times$ 61 cm) optical bench plate (Edmund Scientific) to provide easy, reproducible alignment of the syringe needle and sample target. A removable needle glass syringe (Hamilton Co.) with a volume of 100 μL was chosen for delivering the polymer/matrix solutions. A blunt point stainless steel syringe needle, 5.1 cm long, with an internal diameter of 0.15 mm, was found to work satisfactorily as an electrospray capillary.

The sample target was held on the x-y-z positioner by a magnet mounted in a teflon holder, which electrically insulated the sample target and magnet from the x-y-z positioner and optical bench. A positive DC voltage of approximately 5 kV was applied to the syringe needle, with the sample target and magnetic target holder connected to a ground in common with the ground for the high voltage power supply. Distance from the syringe needle tip to the target was typically 1 to 2 cm. Thin samples were sprayed for approximately

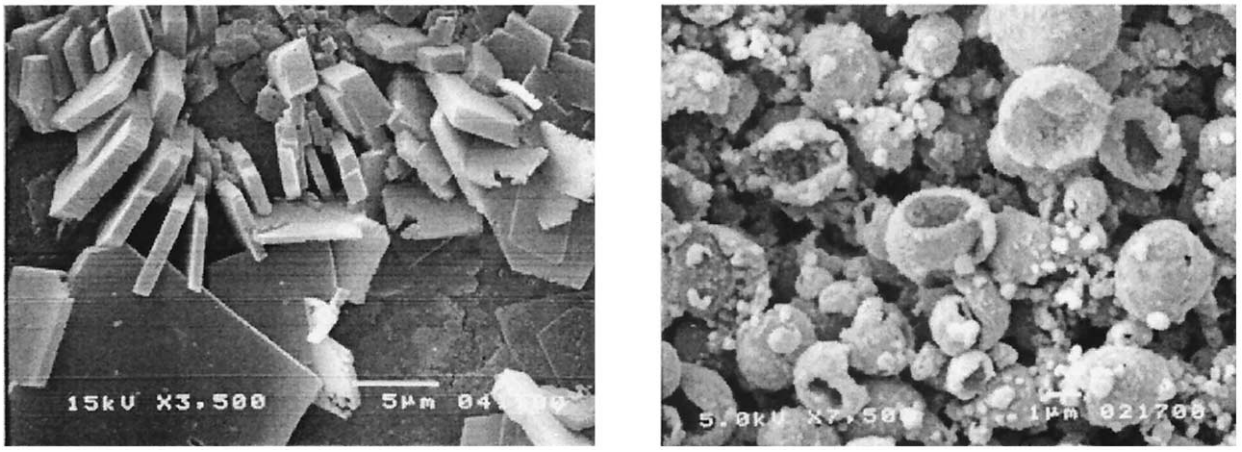

Figure 1. SEM images of a PS 10,200 sample prepared using dithranol as the matrix, silver trifluoroacetate as the ionization reagent and THF as the solvent: (**a**) Dried droplet preparation; (**b**) ES deposition.

30 to 60 s at a flow rate of 2 μL/min. Thick samples were sprayed for 15 to 20 min at a flow rate of 2 μL/min.

Sample Preparation for Azodye Matrix Studies

Samples using azodye matrix compounds were prepared by mixing a saturated solution of the matrix compound in inhibitor-free tetrahydrofuran (THF) in a 1:1 volume ratio with an approx. 0.5 mg/mL poly(ethylene glycol) solution, also prepared in inhibitor-free THF. Matrix solutions were centrifuged (approximately 12,000 $\times$ *g*) for 1 to 2 min to remove any undissolved solids prior to use. For dried droplet samples, approximately 0.5 μL volumes of sample were deposited on the target surface with a glass micropipette. ES-deposited samples were prepared as described above.

Scanning Electron Microscopy

The SEM experiments at Air Products and Chemicals, Inc. (Figures 3, 5, and 6) were conducted using a JEOL JSM-6300 scanning electron microscope equipped with a field emission electron gun. The specimens were analyzed as received (no conductive metal coating was applied). SEM analysis was performed at 2 kV accelerating voltage. Secondary electron images of representative areas were obtained at low magnification ($\times$2000) to show the size distribution of particle clusters, and a higher magnification ($\times$5000) to show the particle morphology. Particle size analysis was performed on a Macintosh computer using the public domain NIH Image program [19].

The MALDI samples examined by SEM at NIST (Figure 1) were given a light, gold coating prior to being placed in the electron microscope. A Denton Vacuum Desk II Cold Sputter/Etch unit (Denton Vacuum Inc., Moorestown, NJ) was operated for 45 s to deposit a gold coating approximately 0.01 μm thick on the samples. A JEOL model 5300 scanning electron microscope was used for all SEM microscopy at NIST. Accelerating voltages of 5 to 15 kV were used with magnification ranging from $\times$3500 to $\times$7500.

Atomic Force Microscopy

Atomic force microscopy (AFM) analysis of the ES-prepared samples was performed on a Dimension 3000 microscope and Nanoscope IIIa controller from Digital Instruments (Santa Barbara, CA). Experiments were run in Tapping Mode, a non-contact mode of AFM, in which the cantilever is oscillated at its resonant frequency, and the feedback is provided by amplitude damping rather than simple deflection. Imaging was done with silicon, 125 μm long tapping tips, with probe apexes of under 20 nm. Ten-micron images were collected at scan rates of 0.5 to 1 Hz. Images are presented as top view images in which point source "illumination" is simulated, and as pseudo 3-D images in which the data are presented as though the surface is viewed obliquely.

Confocal Microscopy

A Zeiss model LSM 510 reflection laser scanning confocal microscope (LSCM) was employed to measure the thickness of several of the "thick" electrosprayed coatings. LSCM illuminates the sample with coherent light and collects light exclusively from a single plane (a pinhole sits conjugated to the focal plane) and rejects light out of the focal plane. The wavelength, numerical aperture (N.A.) of the objective, and the size of the pinhole dictate the resolution in the thickness or axial direction. By moving the focal plane, single images (optical slices) can be combined to build up 3-D stack of images that can be digitally processed.

Mass Spectrometry

The MESIMS experiments were conducted on a Physical Electronics (Eden Prairie, MN) TRIFT II time-of-flight mass spectrometer (TOF MS) equipped with both a ^{69}Ga liquid metal ion gun (600 pA) for Time-of-Flight Secondary Ion Mass Spectrometry (TOF-SIMS) experiments and a N_2 laser (Laser Photonics, 337 nm, 600 ps pulse width) for MALDI experiments [20]. The instrument measures mass via time-of-flight, incorporating both a short linear flight tube and three electrostatic sectors for a curved flight path of approximately 2 m. In TOF-SIMS mode we typically used a 600 pA, 15 kV (14 ns pulse width) bunched primary ion beam for high resolution mass spectrometry, and a 600 pA, 25 kV (20 ns pulse width, 250 nm probe size) unbunched primary ion beam for high lateral resolution ion imaging. Typical mass resolution at 15 kV was 7000 at 100 Da. The lateral resolution is dependent on both the sample and the secondary ion yield. For the experiments at 25 kV, the lateral resolution was typically about 1 to 2 μm. Typical repetition rates were 5 to 15 kHz. Total primary ion doses were less than 10^{12} ions/cm^2. The raster areas varied from 50 $\times$ 50 μm for high resolution imaging to 400 $\times$ 400 μm. The secondary ions were extracted using an electric field imparting 3.2 kV of kinetic energy. Ions experienced 7 kV of post-acceleration just prior to detection. The MCP detector was held at 1400 V. A multistop time-to-digital converter with 138 ps time resolution processed signals from the detector. Data acquisitions for mass spectra averaged between 5 to 10 min and for images averaged between 10 to 20 min.

In static SIMS experiments of insulating samples, surface charging is often a problem. The TRIFT instrument is equipped with a pulsed charge compensator to mitigate this problem. In these experiments, we did not observe any problems with surface charging. Experiments conducted with and without the charge compensator produced the same results. While polymer films can be good insulators, leading to charging problems, the MESIMS samples are thin films primarily composed of matrix with many defects where the underlying metal substrate shows through. Either the access to the metal substrate or the behavior of the matrices apparently solves any surface charging problem [9].

In MALDI mode, the laser was greatly attenuated. Experiments were done with laser fluence slightly above threshold for MALDI. The optical system used on the TRIFT instrument produces a very small laser spot, a circle about 4 μm in diameter. Spectra were obtained from 125 laser pulses. Desorbed ions were extracted with an electric field imparting 3.2 kV of kinetic energy. Ions experienced 7 kV of post-acceleration just prior to detection. Signal from the detector was digitized and averaged in a digital oscilloscope (LeCroy 9350, 2 ns/channel, 200 μs record length, 200 mV sensitivity, and -790 mV offset).

The MALDI signal repeatability experiments were conducted on a Bruker Reflex II TOF-MS (Bruker Daltonics, Billerica, MA), operated in reflectron mode using delayed extraction. Acceleration voltage was 25 kV. The reflectron flight path is approximately 1.7 meters in length, terminating in a microchannel plate detector. Ions were generated by the emission from a pulsed nitrogen laser with a wavelength of 337 nm and pulse duration of approximately 3 ns. A laser pulse energy of approximately 5 μJ was focused over a spot size of 200 $\times$ 50 μm. Laser energy was attenuated to just above the level needed to produce a signal. Polymer spectra were accumulated from 150 laser shots. The estimated standard uncertainty (Type A) [21] of the peak position in a MALDI mass spectrum, from calibration and repeatability studies, is 0.2 u [22].

Results and Discussion

Microscopy of ES-Deposited MALDI Samples

Figure 1 shows SEM images of both a dried droplet and an ES deposited sample. The samples are PS 10,200 (average molecular mass approximately equal to 10,200 Da) prepared with dithranol as the matrix, silver trifluoroacetate as the ionization reagent and THF without preservative as the solvent. The dried droplet sample is crystalline with a significant variety of crystal sizes and sites. The ES sample is composed of individual spheres, some of which appear hollow or broken. The differences in morphology between the dried droplet and electrosprayed samples are striking. The ES sample is relatively uniform while the dried droplet sample is highly heterogenous. To explore how uniform the ES samples are, we analyzed a variety of ES samples with SEM and AFM.

The SEM and AFM data show individual, 1 to 3 μm diameter, round particles in all of the ES deposited samples. Figure 2 shows the top view and 3-D view of AFM data obtained from a sample prepared from PMMA 2900 with DHB as the matrix and methanol as the solvent sprayed from 15 mm. Figure 3 shows low- and high-magnification SEM data from the same sample. We describe this as thick or high-coverage deposition containing individual particles. We interpret the appearance of individual particles to indicate that these particles are essentially dry when they hit the surface. As such, we expect that no significant re-mixing of the ES droplets occurs during spraying or after the spray particles impact the substrate. The SEM data also show these droplets to be predominantly whole, instead of the broken look of many of the particles in Figure 1. The causes of whole-looking versus broken-looking particles are not yet clear, but they may be influenced by the choice of matrix, solvent, and the flow rate of the electrospray deposition.

In an effort to control the dryness of the ES droplets during the deposition, and in turn, control the degree of mixing of the particles after impact with the substrate, we sprayed a number of samples from different needle-to-substrate distances and from a number of solvents.

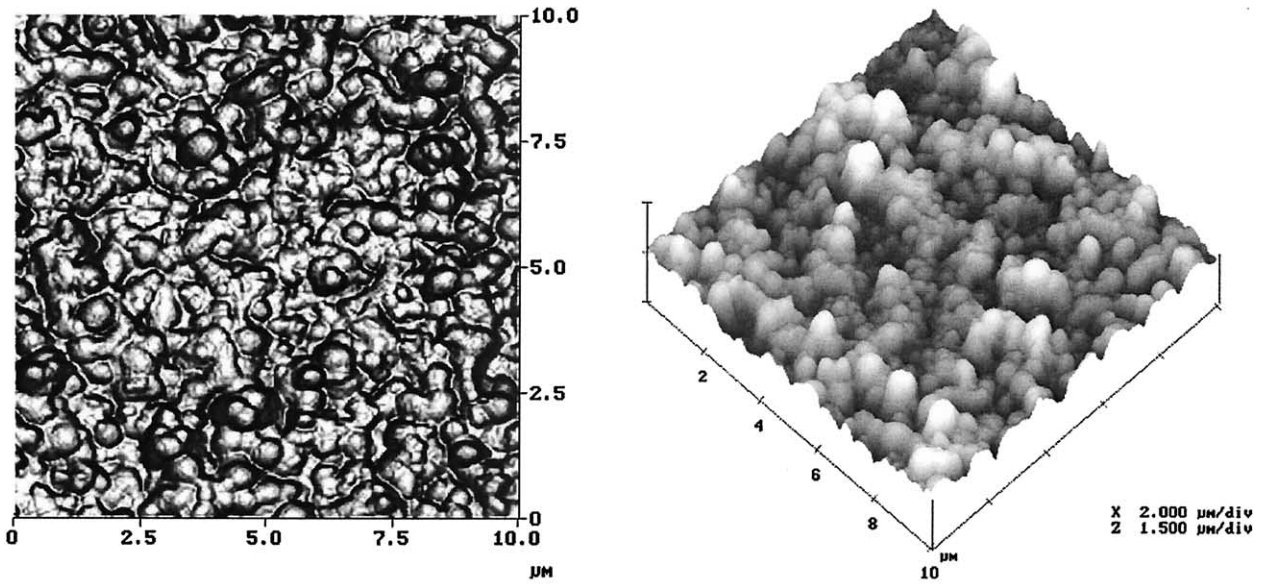

Figure 2. AFM images of a PMMA 2900 sample prepared using DHB as the matrix and methanol as the solvent, electrosprayed from a height of 15 mm.

The spray heights in these studies ranged from 15 to 25 mm. The spray solvents included methanol, acetone, and THF. Figure 4 shows AFM top view and 3-D views of a PMMA sample prepared with DHB as the matrix and acetone as the solvent sprayed from a height of 25 mm. Figure 5 shows SEM low- and high-magnification data for the same sample. While the surface coverage is low (thin electrospray) for this sample, the key features of the particles are essentially unchanged from the 15 mm spray height data shown in Figures 2 and 3. In all of these experiments, the ES deposition produced primarily spherical-shaped particles, which indicates that these are non-interacting particles deposited on the substrate.

The microscopy results suggest that non-interacting particles are deposited during ES deposition, implying that the particles are hitting the substrate almost dry. As noted above, AFM and SEM images provide complementary particle size distribution information. The AFM measures particle height accurately, but because of the finite probe size, cannot measure the particle diameter reliably. The SEM image provides accurate particle diameters, but being essentially a 2-D representation of the surface, does not provide accurate height information. Combining both, we can obtain a complete picture of the particles on the surface of the substrate. Because agglomerations of particles significantly complicate our ability to measure individual particle sizes, we concentrated this effort on the 25 mm spray height data. For the samples shown in Figures 4 and 5, we measured the average width of the particles in the SEM image to be about 250 nm and the average height of the

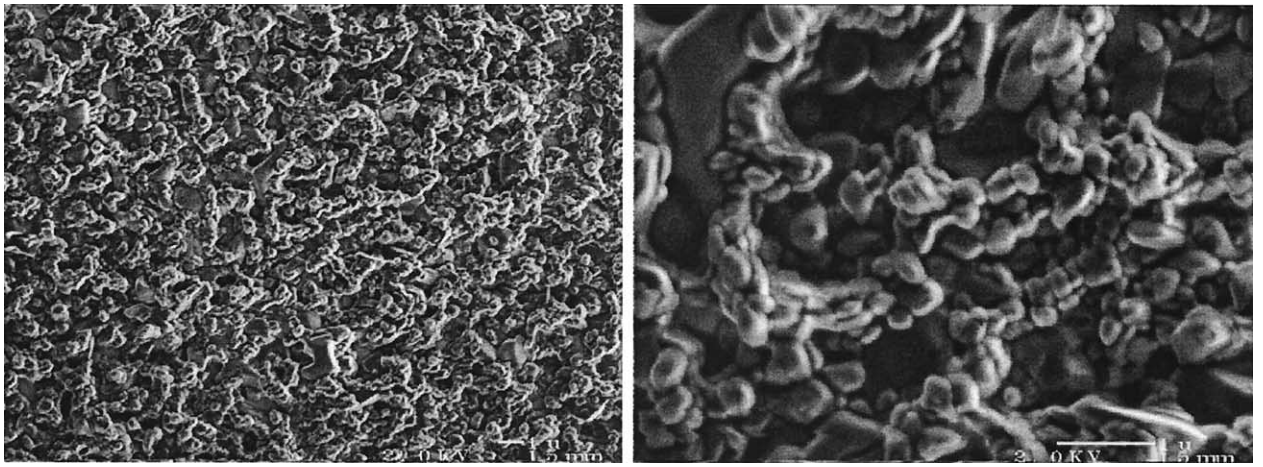

Figure 3. SEM images from a PMMA 2900 sample prepared using DHB as the matrix and methanol as the solvent electrosprayed from a height of 15 mm: (**a**) Low magnification; (**b**) high magnification.

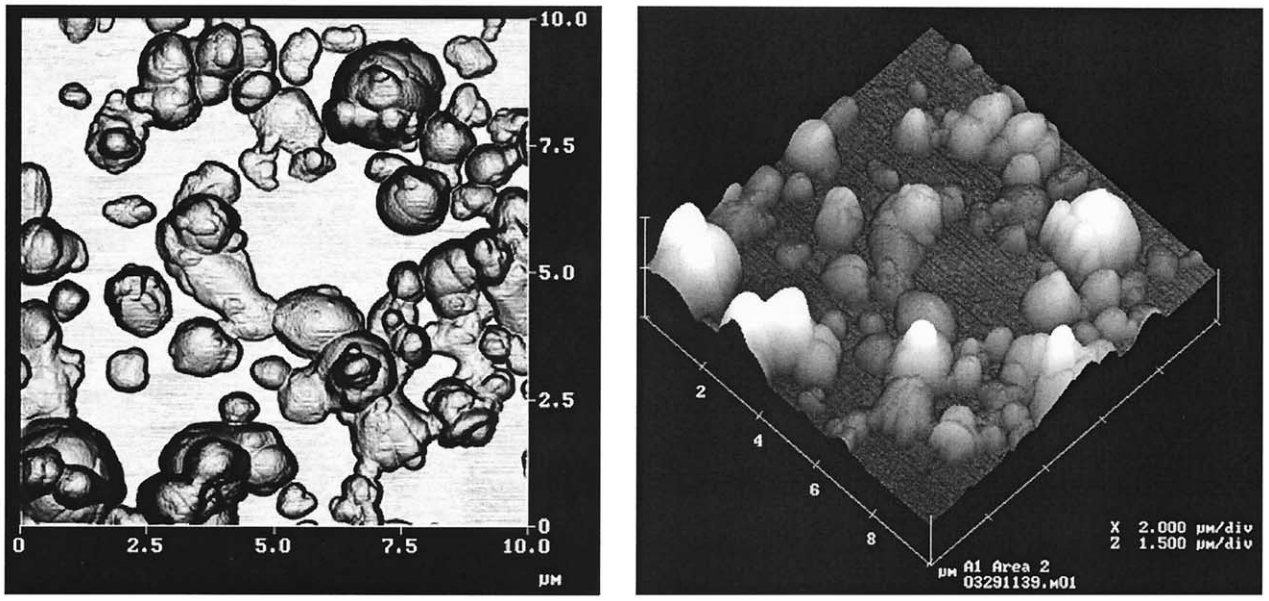

Figure 4. AFM images from a sample of PMMA 2900 prepared using DHB as the matrix and acetone as the solvent, electrosprayed from a height of 25 mm.

particles from the AFM image to be about 170 nm. These data indicate that the particles are significantly flattened on impact. While the particles deform on impact, they remain intact. We interpret this as further evidence that the particles we observe on the target surface are nearly dry before impact. In fact, the similarity between the images obtained with the electrospray needle placed at 15 mm and at 25 mm above the substrate suggests that the drying process is nearly complete very early in the flight of the particles.

As all of the ES-deposited samples have similar morphologies, how can one create morphologies different from the dried droplet yet possessesing some of the homogeneity offered by ES? An example of a different morphology is a sample created by pneumatic nebulization [23]. Figure 6 shows SEM images of a dried droplet sample of DHB and a commercial foil containing DHB from Lab Connections, Inc (Northborough, MA). To the naked eye, the foil sample looks smooth and homogeneous. In the SEM image one can see that the sample contains a large variety of features under a micron in size. The richness of the morphology of the foil may account for its generally high performance in MALDI experiments. These foils are typically used for capturing chromatographic eluents for MALDI analysis [24], but they also work very well as a substrate for dried-droplet sample preparation. We plan to further explore pneumatic nebulization as a method to control the morphology, wetness and re-mixing of a MALDI sample during deposition.

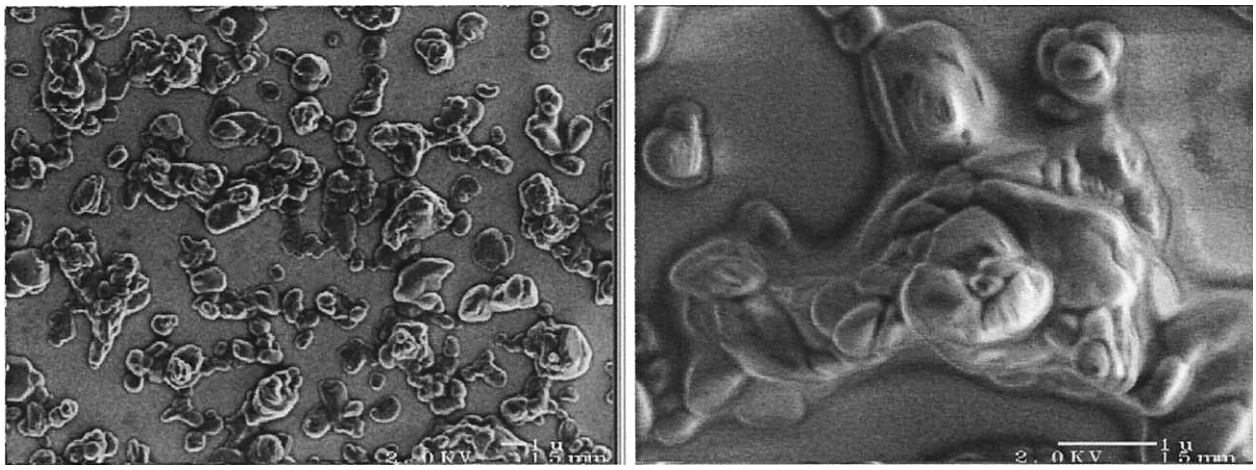

Figure 5. SEM images obtained from a PMMA 2900 sample prepared using DHB as the matrix and acetone as the solvent electrosprayed from a height of 25 mm: (**a**) Low magnification; (**b**) high magnification.

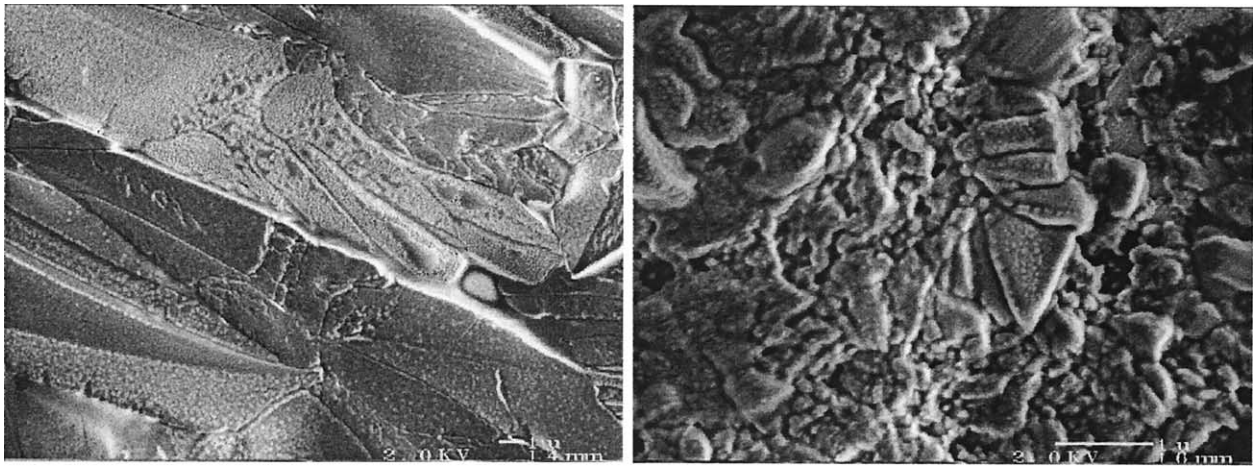

Figure 6. SEM images of DHB matrix prepared by: (**a**) Dried droplet deposition from methanol; (**b**) pneumatic nebulization (a commercial foil produced by Lab Connections, Inc.).

Substrate Coverage of ES-Deposited MALDI Samples

In polymer MALDI of ES samples, we rapidly learned that a thick, higher surface coverage sample produces an improved MALDI signal. The improvements to the MALDI signal include increased longevity in the vacuum chamber, greater signal intensity, and improved precision. The coverage of the ES deposition is dependent on the spray conditions and can change significantly for different solutions. Using MESIMS, we monitor relative spray coverage and determine the spray conditions most likely to give good MALDI mass spectra. Due to the imperfect coverage of the ES-deposited films, some substrate ions are observed by SIMS, even for thickly sprayed samples. By comparing the relative intensities of the matrix ions with the substrate ions, we determine the relative spray coverage for different sprays.

Figure 7 shows a small section of the MESIMS mass spectra from samples of PMMA prepared with DHB matrix and methanol solvent. The three spectra are from samples exposed to ES deposition for 30, 45, and 60 s. The 137, 154, and 155 Da ions are the expected DHB ions, assigned as DHB $-$ H_2O + H^+, DHB^+, and DHB + H^+, respectively. The 141, 142, and 157 Da ions are indicative of the front-coated mirror surface. Interestingly, the front-coated Al mirrors did not have Al or Al oxides on the surface. These ions are most likely from an optical coating applied on top of the Al mirror. Figure 8 shows the decrease in the ratio of the substrate ions to the matrix ions. The lines through the data points are the result of a quadratic fit. The extrapolation of these data indicates that for this solution spray times of about 75 s are required for complete surface coverage. Similar experiments for solutions of PS using IAA and THF extrapolated to about 125 s of spraying required for complete coverage. At this time the optimal spray time needs to be measured for each solution. We

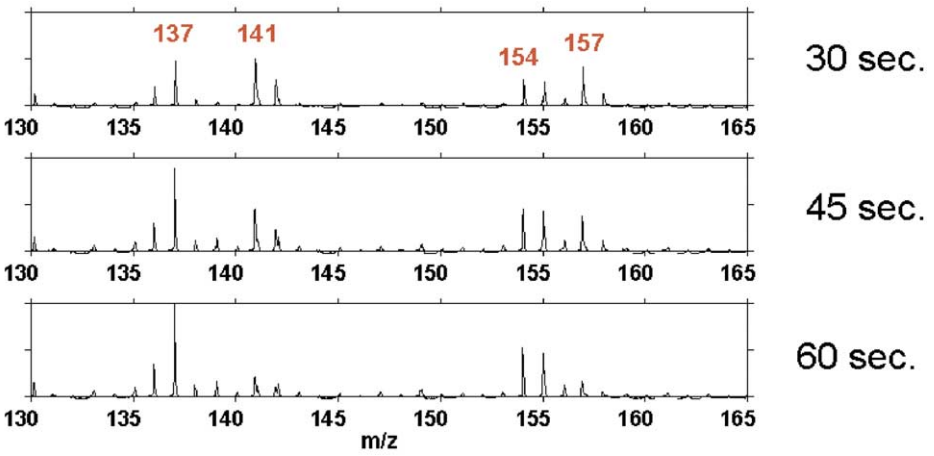

Figure 7. Expansion of an MESIMS mass spectrum showing both matrix (DHB: 137 Da, 154 Da, and 155 Da) and substrate (141 Da, 142 Da, and 157 Da) ions for ES deposited samples prepared from PMMA 2900 and DHB with spray times of: (**a**) 30 s; (**b**) 45 s; (**c**) 60 s.

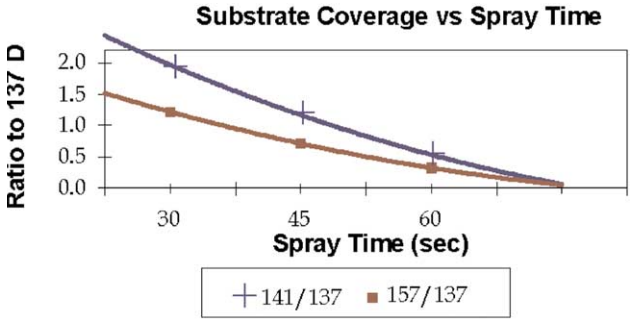

Figure 8. Trends of the ratios of the substrate/matrix ion signals as a function of spray time for the PMMA 2900 sample prepared using DHB: (**a**) 141/137; (**b**) 157/137. The lines correspond to a quadratic fit through the data.

have not yet discovered a meaningful trend in the spray-time data collected.

Layer Deposition by ES

Another interesting parameter of ES deposited samples is the robustness of the layer. Our microscopy data indicate that the sample particles do not interact after deposition. To investigate whether ES can generate intact, non-interacting layers, two-layer samples were created from PMMA prepared with DHB as the matrix and methanol as the solvent; PS was prepared with IAA as the matrix, AgTFA as the cationization aid, and THF as the solvent. Samples with complete coverage were prepared by utilizing the coverage curves discussed above. Figure 9 shows segments of the oligomer region of MESIMS mass spectra from each two-layer sample. In the top spectrum of Figure 9 we see only PMMA + Na^+ ions from a sample with the PMMA layer on top of the PS layer. There is no evidence for PS + Ag^+ ions. In the bottom spectrum of Figure 9 we see the opposite result. We see only the PS ions with no evidence for the PMMA oligomers from a sample with the PS layer on top of the PMMA layer.

When these two-layer samples are analyzed by MALDI, we can see the nature of the layers. Figure 10 shows MALDI mass spectra for the PMMA on top of PS two-layer sample with increasing number of laser shots from a single spot. When we constantly move the laser during the experiment, we obtain a MALDI mass spectrum that essentially matches the MESIMS result. We detect only the PMMA oligomer ions. As we allow the laser to sit in one spot and penetrate the layers, the signal originating in the bottom layer increases. The middle mass spectrum was obtained with 25 laser shots per spot. Despite many reasons why the ion intensities could differ (for example, different molecular mass distributions, desorption, and ionization efficiency), we see similar ion intensities for the two polymers. In the bottom spectrum in Figure 10 the PS ions begin to predominate over the PMMA ions. This spectrum was obtained with only 50 laser shots/spot. These data clearly indicate that we can create layers that can be depth-profiled by MALDI. This experiment was repeated for the other two-layer sample, with PS on top of PMMA, and equivalent results were obtained. The only significant difference was the number of laser shots required to penetrate the layers. The PS on top of PMMA sample required far fewer laser shots to penetrate the layers. This may be indicative of absorbance and ablation differences between the DHB and IAA matrices.

Improving the Precision of MALDI Molecular Mass Determination

To use MALDI data for the determination of a polymer molecular mass distribution (MMD), an average value must be determined from a set of individual MALDI spectra. Correct statistical sampling precludes selecting spectra generated from sample "sweet spots" where signal intensity is very good. Traditional dried droplet MALDI sample deposition can generate variations in signal intensity of 40% and more. As the intensity of the mass peaks are critical to the calculation of the peak areas and other moments of the distributions, we ex-

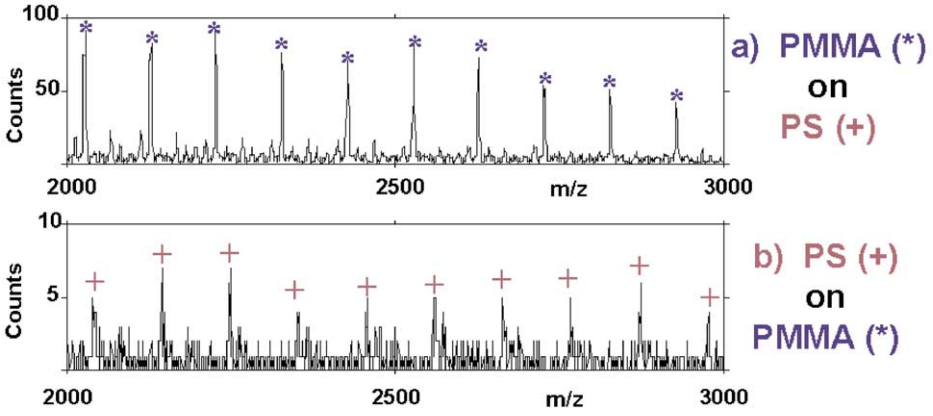

Figure 9. Expansions of MESIMS mass spectra showing oligomer ions obtained from two-layer electrospray deposited samples: (**a**) PMMA on top of PS; (**b**) PS on top of PMMA.

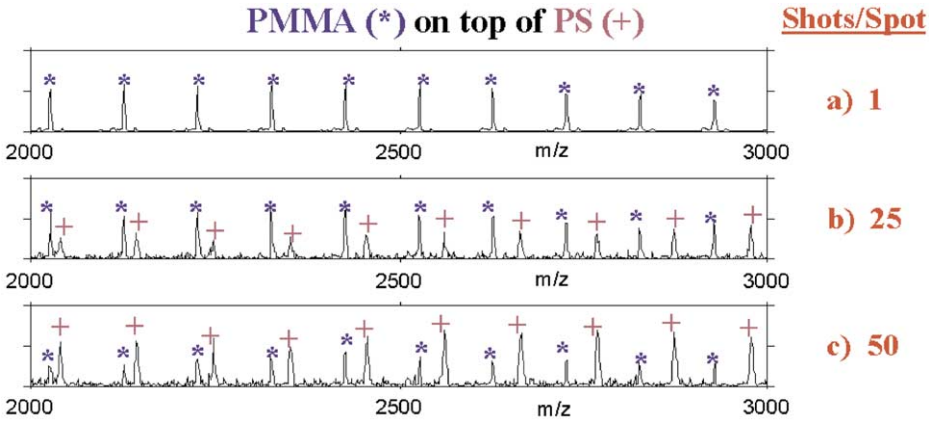

Figure 10. Expansions of MALDI data showing a depth profile through a two-layer sample of PMMA on top of PS taken using: (**a**) 1 laser shot/spot; (**b**) 25 laser shots/spot; (**c**) 50 laser shots/spot.

pected that a signal intensity variation of 40% would be unacceptable for an MMD calculation. This level of variation also raises the question of whether all spectra can be relied on to incorporate the full MMD of the polymer.

Using a series of these specially synthesized azodyes as matrix material and thick electrospray sample deposition, we generated replicate MALDI spectra with variations in the relative integrated peak areas as low as 4.4%, as shown in Table 1. An example MALDI mass spectrum of PEG 1470 analyzed using an azodye matrix is shown in Figure 11. These data show that the electrospray sample preparation technique provides a significant improvement in the consistency of total peak signal integrals compared with a dried droplet deposition.

The data in Table 1 also show that the precision of the MMD calculations (M_N and M_W) significantly improve with the use of electrospray deposition compared to dried droplet deposition. The standard deviation of the M_N and M_W values for the dried droplet experiments are 7.3 and 7.1 Da, respectively. While these values are already much less than the mass of the PEG repeat unit, the ES deposition yields a improvement factor of three in the precision, reducing the standard deviations in M_N and M_W to 2.3 and 2.6 Da, respectively (these values are significant with the one-tailed probability of lower value of F of 0.007 and 0.015, respectively). Interestingly, *t*-tests show that there is a statistically significant difference in the mean of both the M_N and M_W values (the one-tailed probability of a lower *t* is 7.76×10^{-6} and 5.6×10^{-6}, respectively). While these mean values of M_N and M_W are statistically less for the ES deposited samples, the differences are small compared with the mass of a PEG monomer unit. Note that it is the improved precision in the M_N and M_W determinations using ES deposition that enables us to uncover this small but real difference in the mean values of M_N and M_W. The exact cause of the difference in M_N and M_W values determined from the ES and dried

Table 1. A comparison of the total peak area and calculated Mn and Mw values for dried droplet and electrospray sample deposition for PEG 1470 using the azodye matrix from THF solution

Dried droplet preparation			Thick Electrospray preparation		
Peak Area	M_N	M_W	Peak Area	M_N	M_W
440000	1390	1424	1640000	1358.1	1392.5
340000	1391	1426	1590000	1360.2	1391.4
770000	1404	1438	1580000	1361.6	1394.6
790000	1403	1434	1460000	1361.4	1393.0
360000	1406	1441	1620000	1358.2	1389.9
280000	1404	1440	1580000	1364.8	1398.0
690000[a]	*1347*[a]	*1375*[a]	1480000	1360.6	1392.0
$\bar{x}$					
497000	1400	1434	1560000	1360.6	1393.0
s					
225000	7.2	7.1	70000	2.3	2.6
rsd					
45%	0.52%	0.51%	4%	0.17%	0.19%

[a]Both the M_n and M_w values for the sixth dried droplet data point (highlighted) were shown to be outliers using a standard Q-test (tested at the 90% confidence level). These values were excluded from the $\bar{x}$, *s* and rsd calculations shown in the table.

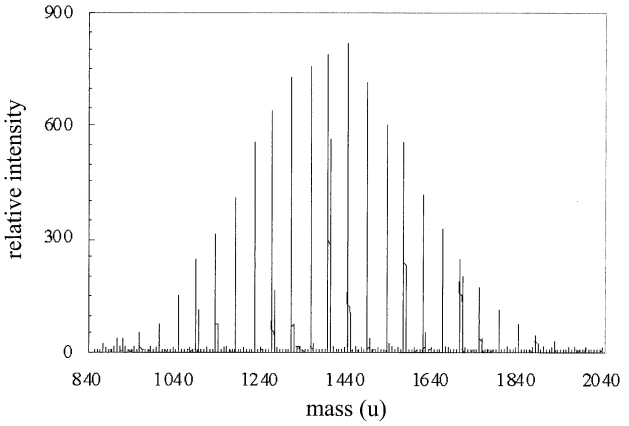

Figure 11. MALDI mass spectrum of PEG 1470 obtained using the azodye matrix.

droplet preparation is not fully understood at this time, but is likely due to small differences in the sample preparation conditions, including the exact matrix-to-analyte ratio [25] and quantity of ionization reagent (cation) present in the sample. This effect is currently the subject of further studies in our laboratories.

Note that the observed improvements in the signal variation are not limited to the azodye matrices. Similar improvements were also produced using more typical MALDI matrices such as DHB and Dithranol. These replicate analyses exhibited small standard deviations in total integrated peak area, M_N, and M_W values as shown in Table 2. The estimated standard uncertainty (Type A) in overall signal intensity, from repeatability studies, varies from 3.2 to 6.5%, depending on the specific sample being analyzed. The precision improvements in the M_N and M_W values also appear to be independent of the analyte polymer and matrix. The systems studied in Table 2 all show very small RSD values, ranging from 0.03 to 0.27%. The increase in overall signal intensity in the Azodye/PEG 1470 data in Table 2 compared with Table 1 is due to changes in the matrix to analyte ratio. These effects are still being studied and will be reported in a future paper.

It was further found that the statistical variation of the peak intensities improved for thick (30 to 40 μL) electrosprayed coatings. Measurement, by confocal microscopy, of a "thick" electrosprayed sample indicated a coating thickness of approximately 170 μm. The same effect was not realized if the electrosprayed coating was thin, prepared using only 2 to 4 μL of matrix/polymer solution. This is because one or two laser shots ablate through a thin sample so the total amount of matrix/polymer ablated varies depending on the film thickness. By making a thick sample coating, abundant polymer signal is typically seen well before laser power reaches a level high enough to ablate through the sample to the underlying target. Consequently, the amount of polymer going into the gas phase is controlled by laser power, which typically varies by 4 to 5% over 150 laser shots.

Table 2. Summary statistics demonstrating the improved reproducibility of electrospray deposited samples for several different analyte and matrix combinations

	PEG 1470/ Azodye	PEG 5000/ DHB	PS 7190/ Dithranol
Number of Spectra	5	8	6
Peak Area Average	350000	2200000	1790000
Peak Area SD	110000	120000	120000
Peak Area RSD	3%	5%	6%
M_N Average	1398	5363.7	6494
M_N SD	3	1.8	18
M_N RSD	0.22%	0.03%	0.27%
M_W Average	1426	5393.4	6638
M_W SD	3	1.9	13
M_W RSD	0.2%	0.04%	0.20%

Conclusions

AFM and SEM images show ES-deposited MALDI samples to be composed of individual, small, nearly round particles. These particles appear to be significantly dry before impact on the substrate and do not appear to interact or re-mix once deposited. The spray thickness was optimized by monitoring the coverage with MESIMS. We also showed that ES-deposited layers are independent and that these layers can be depth-profiled by MALDI by controlling the number of laser shots at each spot.

MALDI data show that thick ES deposited samples produce superior precision for MWD determinations. Using both glassy azodye matrices and ES deposition, we obtain precision on the total counts in a MALDI mass spectrum as low as 3.2% RSD. We also see statistically significant improvement factor of three in the precision of average molecular mass determination. Possible causes of the small though statistically significant decrease in the measured Mn and Mw values for ES versus dried droplet prepared samples are currently under study.

Acknowledgments

The authors thank Air Products and Chemicals, Inc. and the National Institute of Standards and Technology for their support of this research, and Dr. John Sadowski (APCI) for critical review of the manuscript. They also thank Dr. Shashadhar Samal for preparation of the azodye matrix compounds while he was in the Department of Chemistry at Ravenshaw College, Cuttack–753 003, India.

References

1. Tanaka, K.; Waki, H.; Ido, Y.; Akita, S.; Yoshido, Y.; Yoshido, T. Protein and Polymer Analyses up to *m/z* 100,000 by Laser Ionization Time-of-Flight Mass Spectrometry. *Rapid Commun. Mass Spectrom.* **1988,** *2,* 151.
2. Karas, M.; Hillenkamp, F. Laser Desorption Ionization of Proteins with Molecular Masses Exceeding 10,000 Daltons. *Anal. Chem.* **1988,** *60,* 2299.

3. Bahr, U.; Deppe, A.; Karas, M.; Hillenkamp, F.; Giessman, U. Mass Spectrometry of Synthetic Polymers by UV-Matrix-Assisted Laser Desorption/Ionization. *Anal. Chem.* **1992,** *64,* 2866.
4. Hillenkamp, F.; Karas, M.; Beavis, R. C.; Chait, B. T. Matrix-Assisted Laser Desorption/Ionization Mass Spectrometry of Biopolymers. *Anal. Chem.* **1991,** *63,* 1193A.
5. Nielen, M. W. F. MALDI Time-of-Flight Mass Spectrometry of Synthetic Polymers. *Mass Spectrom. Rev.* **1999,** *18,* 309.
6. Hanton, S. D. Mass Spectrometry of Polymers and Polymer Surfaces. *Chem. Rev.* **2001,** *101,* 527.
7. Sperling, L. H. Introduction to Physical Polymer Science; John Wiley and Sons: New York, 1986.
8. Vorm, O.; Roepstorff, P.; Mann, M. Improved Resolution and Very High Sensitivity in MALDI TOF of Matrix Surfaces Made by Fast Evaporation. *Anal. Chem.* **1994,** *66,* 3281.
9. Hanton, S. D.; Clark, P. A. C.; Owens, K. G. Investigations of Matrix-Assisted Laser Desorption/Ionization Sample Preparation by Time-of-Flight Secondary Ion Mass Spectrometry. *J. Am. Soc. Mass Spectrom.* **1998,** *9,* 282.
10. Axelsson, J.; Hoberg, A. M.; Waterson, C.; Myatt, P.; Shield, G. L.; Varney, J.; Haddleton, D. M.; Derrick, P. J. Improved Reproducibility and Increased Signal Intensity in Matrix-Assisted Laser Desorption/Ionization as a Result of Electrospray Sample Preparation. *Rapid Commun. Mass Spectrom.* **1997,** *11,* 209.
11. Hensel, R. R.; King, R. C.; Owens, K. G. Electrospray Sample Preparation for Improved Quantitation in Matrix-Assisted Laser Desorption/Ionization Time-of-Flight Mass Spectrometry. *Rapid Commun. Mass Spectrom.* **1997,** *11,* 1785.
12. Miles, M. J. Scanning Probe Microscopy—Probing the Future. *Science* **1997,** *277(5333),* 1845−1846.
13. Newbury, D. E.; Joy D. C.; Echlin P.; Fiori C. E.; Goldstein J. I. Advanced Scanning Electron Microscopy and X-Ray Microanalysis; Plenum Press: New York, 1986.
14. Wu, K. J.; Odom, R. W. Matrix-Enhanced Secondary Ion Mass Spectrometry: A Method for Molecular Analysis of Solid Surfaces. *Anal. Chem.* **1996,** *68,* 873.
15. Nicola, A. J.; Muddiman, D. C.; Hercules, D. M. Enhancement of Ion Intensity in Time-of-Flight Secondary-Ionization Mass Spectrometry. *J. Am. Soc. Mass Spectrom.* **1996,** *7,* 467.
16. Castle, J. E.; Zhdan, P. A. Characterization of Surface Topography by SEM and SFM: Problems and Solutions. *J. Phys. D: Appl. Phys.* **1997,** *30,* 722–740.
17. Samal, S.; Das, R. R.; Mohapatra, N. K.; Acharya, S.; Dey, R. K. Synthesis, Characterization, and Metal-Ion Uptake Studies of Chelating Resins Derived from Formaldehyde-Condensed Azo Dyes of Aniline and 4,4′-Diaminodiphenylmethane Coupled with Phenol/Resorcinol. *J. Appl. Polym. Sci.* **2000,** *77,* 3128.
18. Szele, I.; Zollinger, H. Azo Coupling Reactions. Structures and Mechanisms. *Top. Curr. Chem.* **1983,** *112,* 1.
19. Software Developed at the U.S. National Institutes of Health and Available on the Internet at http://rsb.info.nih.gov/nih-image/.
20. Schueler, B. Microscope Imaging by Time-of-flight Secondary Ion Mass Spectrometry. *Microsc. Microanal. Microstruct.* **1992,** *3,* 119.
21. Taylor B. N.; Kuyatt, C. E. Guidelines for Evaluating and Expressing the Uncertainty of NIST Measurement Results. *NIST Tech. Note 1297*, September 20, 1994.
22. Wallace, W. E.; Guttman, C. M. Data Analysis Methods for Synthetic Polymer Mass Spectrometry: Autocorrelation. *J. Res. Natl. Inst. Stand. Technol.* **2002,** *107,* 1.
23. Direct Coupling of Size Exclusion Chromatography and MALDI-MS for Polymer Analysis. *Application Note AN-31*; Lab Connections, 10 Bearfoot Rd., Northborough, MA 01532.
24. Hanton, S. D.; Liu, X. M. GPC Separation of Polymer Samples for MALDI Analysis. *Anal. Chem.* **2000,** *72,* 4550.
25. Wallace, W. E.; Guttmann, C. M.; Hanton, S. D. Quantitative Synthetic Polymer Mass Spectrometry Workshop. *J. Res. Natl. Inst. Stand. Tech.* **2003,** *108,* 79.